International Journal of Pressure Vessels and Piping 86 (2009) 563–569

Contents lists available at ScienceDirect

International Journal of Pressure Vessels and Piping

journal homepage: www.elsevier.com/locate/ijpvp

Change in contribution of block boundary to macroscopic strength of 10Cr–1 Mo–1W–VNbN steel due to creep

Motoki Nakajima*, Shin-ichi Komazaki, Yutaka Kohno

Department of Materials Science and Engineering, Muroran Institute of Technology, 27-1 Mizumoto-cho, Muroran, Hokkaido 050-8585, Japan

ARTICLE INFO

Article history:
Received 14 February 2008
Received in revised form
1 June 2008
Accepted 1 June 2008

Keywords:
High Cr ferritic steels
Turbine rotor steel
Creep damage
Indentation test
Block boundary
Locking parameter

ABSTRACT

Outstanding strength performance of high Cr ferritic steels is attributable to the combined strengthening mechanisms of matrix and various grain boundaries. However, it is by no means easy to separate the contributions of such strengthening factors and quantitatively understand them because of extremely fine and complicated microstructures. In this study, the instrumented indentation test was carried out to clarify the change in contribution of "block" during creep. The materials used in this study were turbine rotor steel (Fe–10Cr–1Mo–1W–VNbN). The indentation test was applied to the as-tempered and creep damaged specimens under the maximum loads ranging from 1 to 1000 mN. The test results revealed that the decrease in contribution of block was the predominant factor controlling the material deterioration, namely, softening at the early stage of the creep life. This decrease in block's contribution was caused by the decrease in resistance of the block boundary to deformation.

1. Introduction

The improvement of thermal efficiency in thermal power plants has been currently taken up as important issues worldwide from the perspectives of energy saving, environmental conservation. This improvement can be achieved by elevating an operating temperature and pressure of steam. Advanced 9–12% chromium ferritic steels have been expected to be candidate materials for high-temperature components used in such severe operating conditions [1,2,3], because of their excellent high-temperature strength as well as superior oxidation and corrosion resistances. It is well known that their outstanding strength performance is ascribed to the combined strengthening mechanisms of matrix and various grain boundaries. Fig. 1 shows the schematic illustration of the complex microstructural factors affecting the strengthening mechanisms in martensitic steels. By the normalizing, they obtain a complex lath martensitic structure consisting of several microstructural units, namely, in the order of their size, extremely fine lath, block and/or packet, and prior austenite grain. The block is aggregate of the laths with the same variant. The packet is aggregate of the blocks with the same plane [4]. The lath boundary is a low-angle boundary and the rest are high-angle ones [5,6,7]. Hence the block boundary is considered to be the effective grain boundary in the lath martensite structure and the block subdivided into the laths behaves as a single grain when stressed. Furthermore, the other strengthening mechanisms such as precipitation strengthening attributed to Laves phase, solid-solution strengthening by tungsten and molybdenum, and dispersion strengthening by MX carbonitride contribute to their strength. However, it is very difficult to separate the contributions of such strengthening factors individually and quantitatively understand each contribution because of extremely fine and complicated microstructures. Therefore, the material degradation mechanism of this kind of steel has not been thoroughly clarified [8]. Needless to say, a nondestructive procedure for damage evaluation has not been established as yet [9].

Hirukawa et al. investigated the contribution of block width, solid solution, dislocation, and carbide dispersion to hardness in tempered martensitic steels by using a nanoindentation hardness testing system [10]. By using same technique, Sawada et al. also investigated the contributions of microstructural factors to hardness in normalized, tempered, aged and crept materials of Mod.9Cr–1Mo steel [11]. Jang et al. revealed the contribution of grain boundary to strengthening and aging degradation in advanced 12% Cr ferritic/martensitic steel by using nanoindentation experiments together with microstructural observations [12]. Moreover, Ohmura et al. investigated the contribution of grain (block) boundary to the macroscopic strength of Fe–C binary martensitic steels by the nanoindentation and micro Vickers hardness tests [13,14]. They have successfully separated the contribution of block boundary and concluded that the block

* Corresponding author. Tel.: +81 143 46 5668; fax: +81 143 46 5601.
E-mail address: s1426064@mmm.muroran-it.ac.jp (M. Nakajima).

0308-0161/$ – see front matter © 2009 Elsevier Ltd. All rights reserved.
doi:10.1016/j.ijpvp.2009.04.007

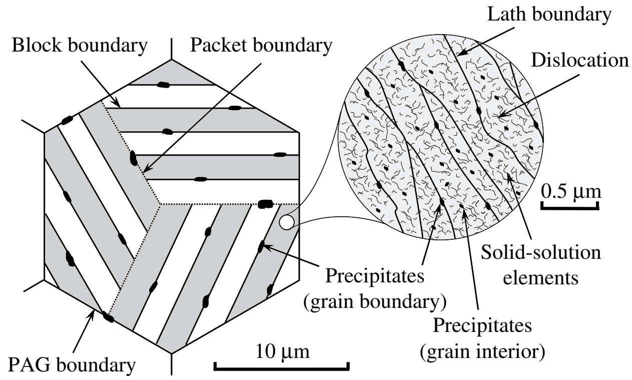

Fig. 1. Strengthening factors of lath martensitic structure.

boundary was the most effective microstructural factor for the macroscopic strength of Fe–C binary martensitic steels.

In this study, the instrumented indentation test was carried out under a wide variety of maximum loads to clarify an effect of block boundary on the strengthening and degradation mechanisms of high Cr ferritic steel. The tests were applied to the gauge and grip portions of creep damaged specimens of 10Cr–1Mo–1W–VNbN turbine rotor steel. The dependence of hardness on maximum load was examined by comparing the sizes of each microstructural factor and the plastic zone under the indenter. Additionally, the change in contribution of block boundary was discussed from the standpoint of the resistance of the block boundary to deformation.

2. Experimental procedures

2.1. Materials and creep specimens

The material used in this study was 10Cr–1Mo–1W–VNbN steel, which has been developed as a steam turbine rotor steel. The chemical composition and heat treatment condition are given in Table 1. The interrupted creep tests were carried out at 650 °C/147 MPa using the as-tempered steel. The tests were stopped at various stages of the life, i.e., 0.5%, 5%, 20%, 40%, 60%, 86% and 100% ($t_r = 564$ h), as indicated in the creep strain rate versus time curve of Fig. 2. The creep rupture test was also performed at 650 °C/98 MPa ($t_r = 4524$ h). The gauge and grip portions of all the specimens were used as the creep damaged and thermally aged specimens respectively.

The changes in lath width and dislocation density inside the lath were determined using transmission electron microscope (TEM) and the inter-particle spacing was also measured by the extraction replica technique. The optical microscopy was performed to measure the block and prior austenite grain sizes quantitatively.

2.2. Instrumented indentation tests

The instrumented indentation test was carried out using the commercialized machine MZT-522 (Mitsutoyo Co.) with a typical three-sided pyramidal Berkovich indenter tip at room temperature. The tests were performed under the maximum indentation loads ranging from 1 to 1000 mN. The duration of loading, holding at each maximum load and unloading were fixed at 100, 10 and 50 s, respectively, irrespective of the test conditions and specimens. The hardness, *H*n, was determined according to the Oliver and Pherr method [15]. More than twenty indentation tests under each testing condition were made on electro-polished samples instead of mechanically polished ones, to avoid artifacts related to a hardened surface layer. The specimen surfaces were initially ground with fine emery paper of #2400 and then electrically polished in a phosphoric acid solution (100 ml) with chromium oxide VI (50 g) at a temperature of 348 K and current density of 0.8 mA/mm^2 for 60 s.

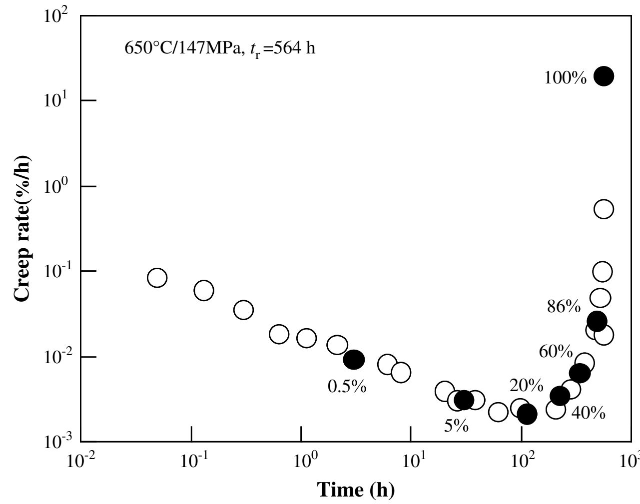

Fig. 2. Creep strain rate plotted as a function of time and conditions of interrupted creep tests.

The plastic zone size under the indenter was estimated based on the Johnson's expanding-cavity model for elastic–plastic indentation with a cone [16] to investigate the contributions of microstructural factors to hardness. The diameter of plastic zone, *b*, was calculated by the following equation.

$$b = a[6(1-\nu)]^{-1}\left[(E/\sigma_{ys})\tan\beta + 4(1-2\nu)\right]^{1/3} \quad (1)$$

where *a* is the diameter of contacted area determined by the Oliver–Pharr method, β is the angle of inclination of the conical indenter to the surface of the edge of indentation, *E* is the Young's modulus (200 GPa), ν is the Poisson's ratio (0.3) and σ_{ys} is the yield strength (710 MPa). To relate this conical indentation model to the present results, we make the usual assumption that similar behavior is obtained when the angle of the cone gives the same area-to-depth relation as the pyramid. For the Berkovich indenter (whose centerline-to-face angle is 65.03°), the equivalent cone angle is 70.03° and thus β is 19.97°. Conventional Vickers hardness measurements were carried out under the load level of 98 N at room temperature, as well as the indentation test.

3. Results and discussion

3.1. Dependence of hardness on plastic zone size

Fig. 3 shows the load-displacement curves of the as-tempered and creep ruptured specimen (650 °C/98 MPa), which were

Table 1
Chemical composition (mass%) and heat treatment condition of turbine rotor steel.

C	Si	Mn	P	S	Ni	Cr	Mo	V	Nb	W	N	Fe
0.14	0.04	0.62	0.007	0.0025	0.70	10.02	0.99	0.19	0.05	1.00	0.037	Bal.

1050 °C × 5 h, O.Q. + 570 °C × 14 h, A.C. + 650 °C × 17.5 h, A.C.